Analytical Biochemistry 495 (2016) 9–20

Contents lists available at ScienceDirect

Analytical Biochemistry

journal homepage: www.elsevier.com/locate/yabio

Bioluminescent kinase strips: A novel approach to targeted and flexible kinase inhibitor profiling

J. Hennek [a, 1], J. Alves [a], E. Yao [b], S.A. Goueli [a, c], H. Zegzouti [a, *]

[a] R&D Department, Promega Corporation, Madison, WI 53711, USA
[b] SignalChem Pharmaceuticals, Richmond, British Columbia V6V 2J2, Canada
[c] Department of Pathology and Laboratory Medicine, University of Wisconsin School of Medicine and Public Health, Madison, WI 53705, USA

ARTICLE INFO

Article history:
Received 6 October 2015
Received in revised form
11 November 2015
Accepted 16 November 2015
Available online 25 November 2015

Keywords:
Kinase profiling
Bioluminescence
ADP detection
Selectivity profiles
Kinase assay
Kinase inhibitor

ABSTRACT

In addition to target efficacy, drug safety is a major requirement during the drug discovery process and is influenced by target specificity. Therefore, it is imperative that every new drug candidate be profiled against various liability panels that include protein kinases. Here, an effective methodology to streamline kinase inhibitor profiling is described. An accessible standardized profiling system for 112 protein kinases covering all branches of the kinome was developed. This approach consists of creating different sets of kinases and their corresponding substrates in multi-tube strips. The kinase stocks are pre-standardized for optimal kinase activity and used for inhibitor profiling using a bioluminescent ADP detection assay. We show that these strips can routinely generate inhibitor selectivity profiles for small or broad kinase family panels. Lipid kinases were also assembled in strip format and profiled together with protein kinases. We identified two specific PI3K inhibitors that have off-target effects on CK2 that were not reported before and would have been missed if compounds were not profiled against lipid and protein kinases simultaneously. To validate the accuracy of the data generated by this method, we confirmed that the inhibition potencies observed are consistent with published values produced by more complex technologies such as radioactivity assays.

Kinases, one of the largest enzyme families in the cell, represent important biological intersections in signaling pathways [1]. By phosphorylating a diverse array of substrates of various chemical natures (e.g., proteins, lipids, sugars), kinases catalyze the largest number of post-translational protein modifications (PTMs); it has been reported that more than 75% of PTMs are phosphorylations [2]. Kinases orchestrate a multitude of biological processes such as cellular growth, division, and differentiation [1–3]. As a corollary, disruption of these biological processes due to abnormal kinase activity can have a deleterious effect on the cell, leading to serious diseases such as cancer, inflammation, and diabetes. For nearly two decades, kinases have been one of the most targeted enzyme groups in drug discovery research [4,5]; some 30 kinase-based drugs have been approved by the U.S. Food and Drug Administration (FDA), and many are currently undergoing development or in clinical trials [5,6].

In 2001, Gleevec (against ABL kinase) was the first kinase inhibitor approved to treat a cancer, chronic myelogenous leukemia [7]. It became a promising proof of concept that drugs could also be developed against other diseases involving dysregulated kinase activity. Although many kinases were validated as drug targets for a variety of diseases, the majority of approved kinase inhibitor drugs up to now are for treating different types of cancer; only three have been approved for non-oncological diseases. For example, myelofibrosis, rheumatoid arthritis, and idiopathic pulmonary fibrosis are treated with the kinase inhibitors ruxolitinib (JAK1/2), tofacitinib (JAK3), and nintedanib (VEGFR, FGFR, and PDGFR), respectively [8–10]. If success in developing kinase inhibitor drugs has been limited, one reason is that the majority of inhibitors bind to the evolutionary conserved ATP binding pocket common to all kinases. Therefore, it is challenging to identify highly selective inhibitors that will not inhibit off-target kinases and affect other crucial signaling pathways leading to side effects when used as a therapy.

Abbreviations used: PTM, post-translational modification; FDA, U.S. Food and Drug Administration; BSA, bovine serum albumin; DMSO, dimethyl sulfoxide; TK, tyrosine kinase families; CMGC, protein kinase CDK; MAPK, GSK3, and CLK families; CDK, cyclin-dependent kinase; TKL, tyrosine kinase-like families; HTS, high-throughput screening; CK, casein kinase families.

* Corresponding author.
E-mail address: hicham.zegzouti@promega.com (H. Zegzouti).
[1] Current address: Exact Sciences, Madison, WI 53719, USA.

http://dx.doi.org/10.1016/j.ab.2015.11.007

Reduced selectivity may be a lesser concern when treating cancer given that some off-target effects may be tolerated for the greater benefit of the therapy [11]. However for nonlethal maladies, high target selectivity is critical for avoiding side effects due to drug toxicities that could outweigh the therapeutic benefits of the drug and cannot be managed. This could explain why the majority of the drugs approved are for the treatment of cancer. Many pharmaceutical companies endeavor to develop drugs that have the right balance between potency and selectivity for cancer and for other ailments [5] such as chronic inflammatory and autoimmune diseases [12], hypertension, and Parkinson's disease [13].

Many drug discovery programs are devoted to the identification of kinase inhibitors with an adequate balance between potency and selectivity. To achieve this balance, new drug entities need to be profiled against various liability panels including protein kinases. Profiling a compound against a broad panel of kinases provides a better understanding of its mode of action and may reveal potential toxicities [14,15]. Moreover, defining specificity of inhibitors toward a particular kinase or kinase group has proved to be useful to the research community in general and to the cell-signaling community in particular [16,17].

Several kinase detection assays have been developed for kinase–small molecule interactions in low-to high-throughput settings [18–21]. These technologies are used either to measure the effect of the small molecule on the catalytic activity of the kinase or to assess the binding affinity to the ATP binding pocket. Although these assays are classically used for a small number of kinases at a time in a screening or characterization mode, they are mostly deployed for profiling in a fee-for-service model by service providers [22–27]. Some offer large kinase panel profiling using activity-based radiometric assays [23,26]. Others use phage display-based binding assays because they provide large kinase panel profiling service [24,25]. Other technologies, such as mobility shift kinase assays, were also adopted by others to provide large kinase panel profiling service. This fee-for-service model is attractive given the difficulty of setting up large profiling kinase panels. However, although cost, time, and confidentiality factors may prohibit the use of a service provider, the alternative of creating and maintaining kinase panels in-house may also be cost prohibitive and cumbersome. It would involve rigorously optimizing each enzyme across the panel and keeping a large number of kinase stocks in a perfect stable condition to be used each time a compound selectivity profile is needed [28–30].

In this article, we describe the development of a pre-configured and standardized kinase profiling system that can be implemented as a cost-effective in-house approach. The system is based on luminescent ADP detection by the ADP-Glo kinase assay, a universal platform that has been validated with a large number of kinases for drug discovery, enzyme characterization, and inhibitor mode of action studies [19,31–36]. The kinase profiling systems are a set of kinases presented in one-time-use multi-tube strips containing eight enzymes each with their corresponding substrate strips and are standardized for optimal kinase activity. The strip system provides flexible kinase inhibitor profiling because each strip can be used to profile compounds at a single dose or to create a dose range against eight kinases at once. We created a profiling panel containing 112 kinases belonging to all kinase branches of the kinome [1]. We show that this kinase profiling strip approach can routinely generate selectivity profiles against small or large kinase panels and can identify compound promiscuity across the kinome.

Finally, because chemical compounds specific for one class of kinases such us lipid kinases can potentially have off-target effects and inhibit kinases in other groups of the kinome, we also assembled four class I PI3 kinases in strip format and tested them in an inhibitor profiling experiment. When these were used with protein kinases in the same profiling experiments, unknown off-target effects of specific PI3 kinase inhibitors were identified, emphasizing the importance of profiling lipid and protein kinases simultaneously.

Materials and methods

Materials

Kinases, substrates, and cofactors were obtained from SignalChem (Richmond, BC, Canada), except PKA, PKC, DNA-PK, PI3 kinases α, β, γ, and δ, neurogranin, kemptide, and DNA-PK peptide, which were obtained from Promega (Madison, WI, USA). Table S1 in the Online Supplementary Material provides a list of all the kinases, substrates, and cofactors used in this study. SB203580 was obtained from Promega. Gefitinib, roscovitine, dasatinib, tofacitinib, tozasertib, LY294002, AZD6482, AS252424, and AS605240 were purchased from LC Laboratories (Woburn, MA, USA). The ADP-Glo kinase assay was obtained from Promega. Low-volume, 384-well, white round-bottom untreated polystyrene microplates and half-area 96-well white untreated microplates were obtained from Corning (Corning, NY, USA). Bovine serum albumin (BSA; blot-qualified BSA, cat. no. 3841) was obtained from Promega.

Kinase assay conditions

All kinase reactions were performed in kinase reaction buffer (40 mM Tris [pH 7.5], 20 mM $MgCl_2$, 0.1 mg/ml BSA, and 50 μM dithiothreitol) supplemented with 10 μM ATP and various cofactors (Table S1). All kinase reactions were performed in a 5-μl volume in 384-well plates and were incubated for 1 h at room temperature (22–25 °C).

Kinase and substrate strip assembly

All of the kinases were serially diluted starting from 200 ng per reaction with their substrate and cofactors (concentrations indicated in Table S1). Once optimal kinase concentration was defined, the kinases were diluted in a kinase storage buffer to make a 50× concentrated stock and the substrates/cofactors were diluted to make a 3.3× concentrated stock. These kinases and substrates were grouped by kinase family, assembled in multi-tube PCR strips (eight kinases or eight substrates per strip), and stored at −80 °C as one-time-use aliquots. The kinase and substrate aliquots are 5 and 45 μl per tube, respectively.

Kinase profiling system general protocol

Each kinase stock in the kinase strip was diluted with 95 μl of 2.5× kinase reaction buffer, and each substrate/cofactor stock in the substrate strip was diluted with 15 μl of 100 μM ATP. Both kinase and substrate/cofactor concentrations are now 2.5×. As described in Fig. 3 (see Results and Discussion), 2 μl of the kinase working stocks and 2 μl of the ATP/substrate working stocks were dispensed in the 384-well plate wells along with 1 μl of buffer, compound, or 5% dimethyl sulfoxide (DMSO; vehicle) in a buffer. The reactions were incubated for 1 h at room temperature. To detect the activity of each kinase, the ADP-Glo kinase assay was used according to the manufacturer's protocol and previously published method [19]. Briefly, to the 5-μl kinase reactions, 5 μl of ADP-Glo reagent was added to stop the kinase reaction and deplete any ATP remaining. The mixture was incubated for 40 min at room temperature. Then, 10 μl of kinase detection reagent was added and the mixture was incubated for an additional 30 min to convert the kinase-produced ADP to ATP and then to light using

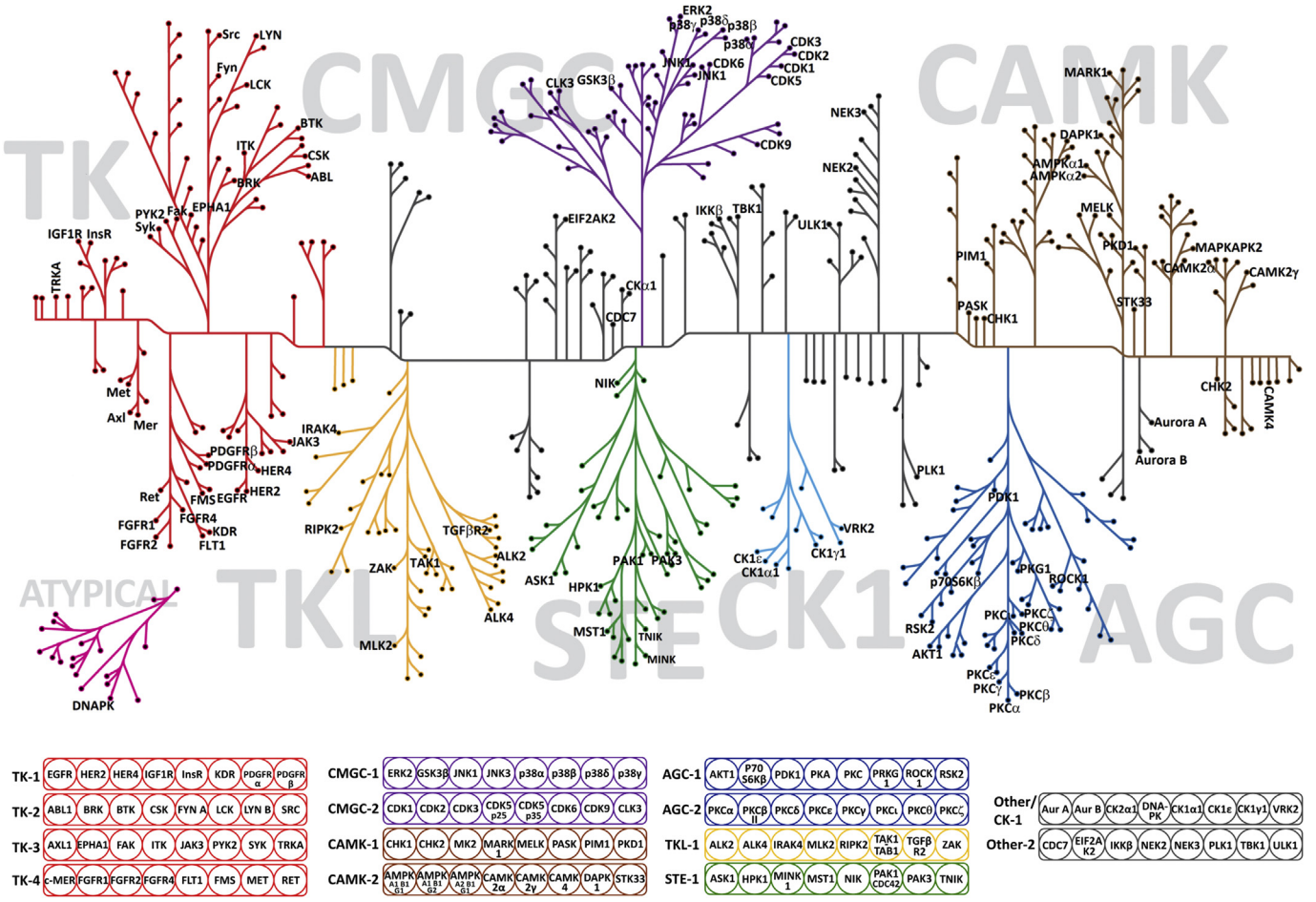

Fig.1. Kinase targets selected for the kinase profiling panel. The kinases are presented on a kinome dendogram based on their relationships in terms of sequence homology and for visualization of the groups to which they belong. Each kinase group is represented with a different color (e.g., red for TK [tyrosine kinase] group) except that the "Other" group kinases spread all over the kinome have a gray color. The bottom panels represent how the 112 kinases are organized in the 14 eight-strip tubes.

luciferase/luciferin reaction. The light generated was measured using a luminometer (GloMax Discover, Promega). The luminescent signal generated is proportional to the ADP concentration present, and it is correlated with the amount of kinase activity. More details about the ADP-Glo assay protocol and its applications were described previously [19].

Kinase inhibitor profiling

Six compounds were used to validate the profiling system's ability to accurately create kinase inhibition profiles. The systems were tested with inhibitors as a single-dose inhibition or in dose–response mode to calculate percentage activity remaining after incubating with one inhibitor dose or to calculate IC_{50} values for eight enzymes at a time. Step-by-step profiling methods described previously, and illustrated in Figs. S1 and S2 in the Supplementary Material, were followed [37]. Briefly, kinase assays were assembled using 1 μl of 5× concentrated compound, 2 μl of kinase working stock, and 2 μl of the corresponding ATP/substrate working stock in a 384-well plate. The volumes aliquoted in the kinase profiling strips are sufficient for either one 10-point inhibitor dose response or up to 10 compounds tested at a single dose. In every experiment, no-enzyme and no-compound control reactions were included to represent background luminescence (0% activity) and non-inhibited kinase activity (100% activity), respectively. The reported percentage kinase activity was calculated by subtracting the average no-enzyme control luminescence from all kinase-containing reactions with or without compound and then converting these net luminescence values to percentage activity based on the no-compound control reactions representing 100% kinase activity.

Results and discussion

To profile a small molecule kinase inhibitor using an activity-based kinase assay, different kinases are simultaneously assayed in the presence and absence of the compound to be profiled. First, an assay that is compatible with all of the kinases to be profiled is selected. Second, prior to profiling, a titration of each enzyme is used to select an appropriate amount to be used in the profiling reactions. This amount of kinase should be as low as possible, in the linear range of the enzyme activity and the assay, and should produce a reasonable assay window (e.g., signal-to-background ratio ≥10). This can reasonably managed with a small number of kinases [29]. However, for large kinase panels or for repetitive routine profiling, the logistics of maintaining enzyme stocks and assay optimization become cost and labor intensive [28,30]. Therefore, we standardized the kinases for activity and created one-time-use kinase and substrate stocks that can be stored in the freezer with stable activity over time. The amounts chosen for each kinase produce similar signal-to-background ratios across the panel to create meaningful inhibitor potency comparisons. In

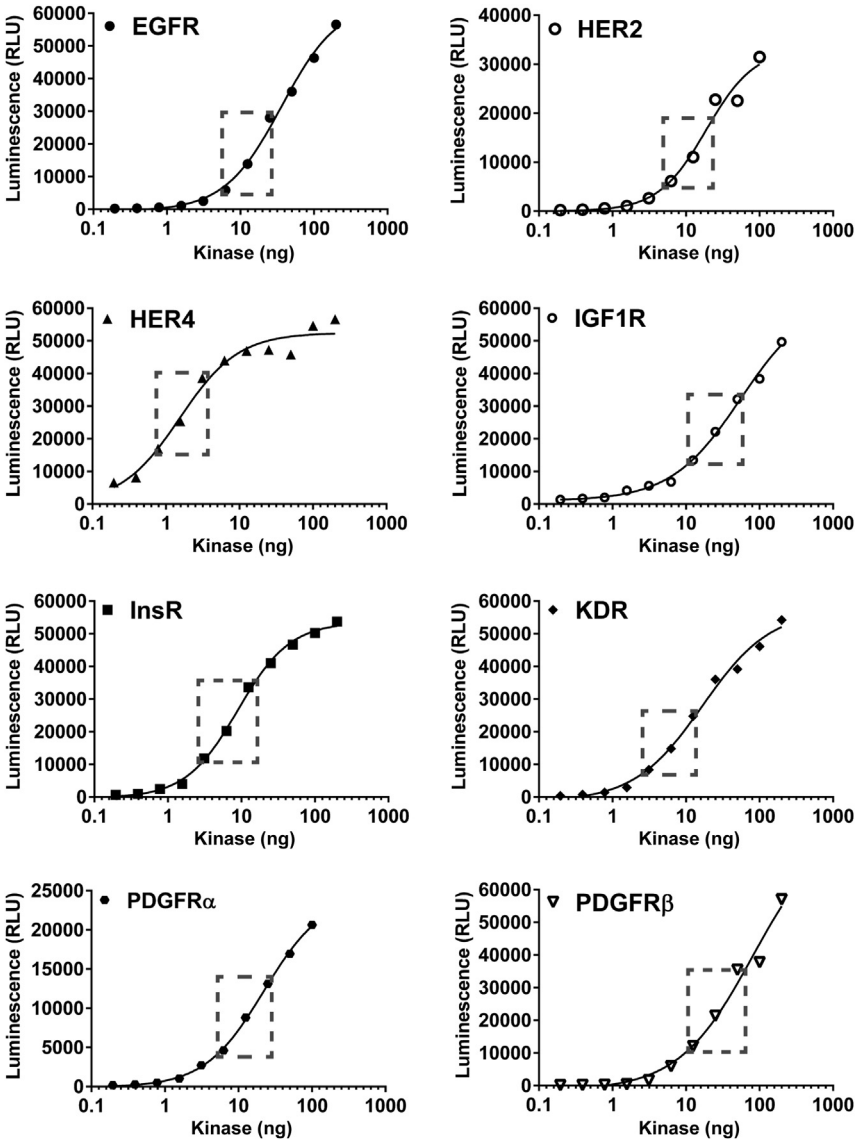

Fig.2. Standardizing kinase activities. Kinases were titrated eight at a time in 384-well plates using a 5-μl reaction volume, and their activities were analyzed using ADP-Glo assay as described in Materials and Methods. The dashed insets represent the linear area of each kinase curve where the amount selected for each enzyme produces approximately 10–30% ATP to ADP conversion with at least a signal-to-background ratio of 10 at 10 μM ATP. Curve fitting was performed using a sigmoidal dose–response (variable slope) equation in GraphPad Prism software. An ATP-to-ADP conversion curve in the 10 μM total nucleotide concentration was performed at the same time to correlate the percentage ADP produced to each RLU (relative light units) value as described previously [19]. Luminescence values represent the averages of two replicates.

addition, to streamline the process, we created a simple protocol with a small number of dispensing steps.

Kinase selections and grouping

To create a meaningful kinase profiling panel, at least eight representative kinases from each branch of the kinome were selected. This provided at least one multi-tube strip containing eight kinases from each subfamily (Fig. 1). The 112 kinases depicted in Fig. 1 and grouped in 14 strips constitute a panel that covers the human kinome in a representative fashion and contains the majority of drug targets identified to date. In addition, the kinases in each branch of the kinome were chosen based on published panels used for profiling during the last decade. The kinases selected have been either commonly profiled in the literature or described in different kinase drug discovery programs [5,28,38]. We included kinase targets of the majority of FDA-approved kinase inhibitors [6] that may serve as inhibition controls (Table 1).

Standardizing kinase activities

Available recombinant kinases have a wide range of specific activities, such that different volumes need to be dispensed from each kinase stock to generate similar activities across a set. To facilitate this process, we chose an amount of each enzyme that converts approximately 10–30% ATP to ADP and produces a signal-to-background ratio of at least 10 at 10 μM ATP. Based on this amount of kinase, stock solutions were created in equal volumes so that after a standardized dilution step, 2 μl of each kinase could be used for each reaction.

The selected enzymes were titrated, eight at once starting from 200 ng per reaction, using assay conditions that we developed previously to create 174 kinase enzyme systems

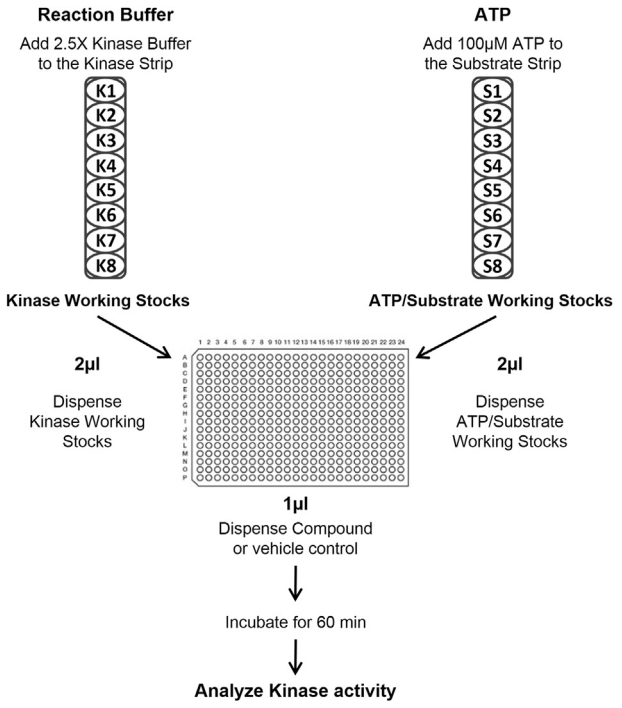

Fig.3. Kinase profiling systems principle. Kinase stocks (50×) were diluted directly in the strip tubes with 2.5× kinase buffer, and substrates/cofactor stocks (3.3×) were diluted with 100 μM ATP solution to create working stocks (2.5×). Kinase reactions were performed using 1 μl of compound or vehicle control, 2 μl of kinase working stock, and 2 μl of ATP/substrate working stock. After a 1-h incubation at room temperature (22–25 °C), kinase activity was quantified using the ADP-Glo kinase assay. The luminescent signal generated is proportional to ADP concentration and is correlated with kinase activity.

(http://www.promega.com/kinase). Fig. 2 shows the titration of eight kinases from the TK family and indicates the optimal curve segments. As an example, the amount chosen from this segment of the EGFR curve is represented in bold in Table 2 (e.g., 12.5 ng/5 μl reaction). Because the kinases are sensitive to freeze/thaw cycles and can lose activity when stored at low concentrations, a 50× concentrated stock of the amount identified by titration was prepared in a storage buffer containing BSA and glycerol. For the EGFR example, the 50× stock is 125 ng/μl, which is aliquoted to 5 μl per strip tube and used one time to create multiple profiling reactions. The volumes aliquoted in the kinase profiling strips (5 μl) are sufficient for either one 10-point inhibitor dose response or up to 10 compounds tested at a single dose, and it is a one-time-use aliquot. It should be noted that dispensing less than 5 μl of kinase stock in the kinase profiling strips could decrease accuracy and reproducibility of the technique. Thus, a drawback of one-time use of the kinase strip could be that if fewer than 10 compounds are to be tested at once in a single-dose experiment, the remaining reconstituted kinase working solution cannot be refrozen and would go to waste.

The substrate and cofactor concentrations are based on assays developed previously and can be stored in a more diluted state than the kinases. The substrate and cofactor mixtures were shown to be stable in −80 °C storage (data not shown). Therefore, we mixed the substrate peptides or proteins and any needed cofactors such as $MnCl_2$, AMP, and lipids to make 3.3× concentrated stocks (see Table S1 in Supplementary Material) and dispensed 45 μl per strip tube. Each eight-kinase strip was paired with its corresponding substrate/cofactor strip and stored at −80 °C.

For ease of use, the profiling protocol was also standardized (see Fig. 3 below) so that only one dilution each is required for the kinase and the substrate stocks to create working solutions. Each kinase and substrate stock is diluted with the same volume of

Table 1
FDA-approved small molecule drugs and their kinase targets present in the profiling system panel described here.

Drug	Year approved	Known target(s)[a,b]	Profiling family strip(s)
Afatinib	2013	**EGFR**	TK-1
Axitinib	2012	**VEGFR1**/2/3 (**FLT1**)	TK-4
Bosutinib	2012	**ABL, SRC, LYN,** HCK	TK-2
Cabozantinib	2012	**RET, MET, VEGFR1**/2/3, **AXL,** KIT, TRKB, FLT3, TIE2	TK-4, TK-3
Ceritinib	2014	ALK, **IGF1R, InsR,** ROS1	TK-1
Crizotinib	2011	ALK, **c-MET,** ROS	TK-4
Dasatinib	2006	**ABL, SRC, LCK, FYN, PDGFRb,** YES, KIT, EPHA2	TK-2, TK-1
Dabrafenib	2013	B-RAF	N/A
Erlotinib	2004	**EGFR**	TK-1
Gefitinib	2003	**EGFR**	TK-1
Ibrutinib	2013	**BTK**	TK-2
Idelalisib	2014	**PI3Kδ**	PI3K small panel
Imatinib	2001	**ABL, PDGFR,** KIT	TK-2, TK-1
Lapatinib	2007	**EGFR; HER2**	TK-1
Lenvatinib	2015	**VEGFR, FGFR, RET, PDGFR,** KIT	TK-4, TK-1
Nilotinib	2007	**ABL, PDGFR**	TK-2, TK-1
Nintedanib	2014	**VEGFR, FGFR, PDGFR**	TK-4, TK-1
Palbociclib	2015	**CDK4/6**	CMGC-2
Pazopanib	2009	**VEGFR, FGFR1/3, FMS, PDGFR,** KIT, **LCK, ITK**	TK-4, TK-1, TK-2, TK-3
Ponatinib	2012	**ABL** and ABL T315I, **VEGFR, PDGFR, FGFR, SRC,** KIT, **RET**	TK-2, TK-4, TK1
Regorafenib	2012	**VEGFR, ABL,** B-RAF, KIT, **PDGFR, RET, FGFR1/2,** TIE2	TK-4, TK-2, TK-1
Ruxolitinib	2011	JAK1/2	N/A
Sorafenib	2005	RAF, KIT, FLT3, **RET, VEGFR, PDGFR**	TK-4, TK-1
Sunitinib	2006	**PDGFR, VEGFR,** KIT, FLT3, CSF-1R, **RET**	TK-1, TK-4
Tofacitinib	2012	**JAK3**	TK-3
Trametinib	2013	MEK1/2	N/A
Vandetanib	2011	**EGFR, VEGFR, RET, BRK,** TIE2, **EPHA, SRC family**	TK-1, TK-4, TK-2, TK-3
Vemurafenib	2011	A/B/C-Raf, B-Raf (V600E)	N/A

[a] The targets shown here are primary and secondary for each drug.
[b] The targets included in the profiling systems are shown in bold.

Table 2
EGFR titration to define 50× concentration for profiling system development.

EGFR (ng)[a]:	200	100	50	25	12.5	6.3	3.1	1.6	0.8	0
RLU	56555	46326	36021	28000	13879	5887	2506	1072	568	158
S/B	358	293	228	117	88	37	16	7	4	1
% ADP	88	73	58	46	22	9	4	2	1	0

Note. RLU, relative light units; S/B, signal-to-background ratio.
[a] The optimal amount chosen for EGFR from the curve is represented in bold.

buffer or ATP. The working solutions become 2.5× concentrated and are ready to be added to the kinase reaction. Because the kinases were standardized for activity in 5-µl reactions, identical volumes of both kinase and substrate working solutions (2 µl each) are added across the plate to create a 1× reaction concentration after 1 µl of buffer, compound, or vehicle (e.g., DMSO) is added to the well. The incubation time was also standardized to 1 h to allow all of the kinases to generate similar percentage ATP conversion.

To test the consistency of our approach, multiple 50× and 3.3× stocks of kinase and substrate strips, respectively, were made, and their performances were compared with each other and with initial pilot stocks following the same protocol. Fig. 4 shows a comparison between the performances of two stocks for eight kinases from the CMGC family strip in terms of luminescence signal and signal-to-background ratio. It shows that the stocks made and frozen over time generated similar data in the previously specified activity range. Multiple additional stocks that were generated showed consistent performance and were stable for at least 9 months to 1 year at −80 °C (data not shown). This demonstrates the validity of this approach for developing profiling reagents in a large stock to be aliquoted and used routinely.

Validating kinase profiling systems with known inhibitors

We showed that consistent kinase activity measurement from the kinase profiling systems can be obtained. To validate the utility of our system for inhibitor profiling, we created single-dose and dose–response inhibition profiles following the protocol described in Fig. 3 and in Figs. S1 and S2 of the Supplementary Material. For single-dose inhibition, four strips of eight kinases were used with five known small molecule kinase inhibitors, either approved drugs or research compounds. A single-dose profiling protocol described in Fig. S1 was used, and we generated data representing percentage

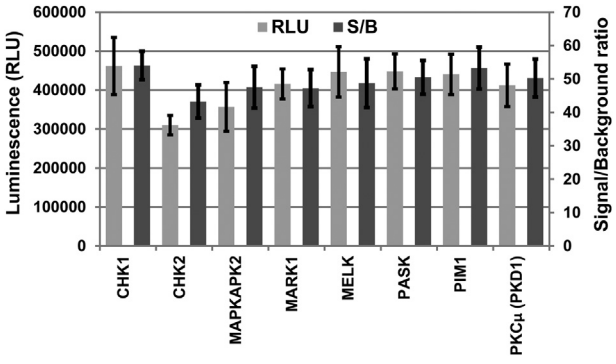

Fig.4. Reproducibility of the kinase strip approach. Two independently made kinase stock batches (50×) of eight kinases from the CMGC group were created according to the described protocol and stored at −80 °C. The activities of both kinase sets were tested using the strip protocol and compared. Luminescence (relative light units, RLU) and signal-to-background (S/B) ratios shown are averages of replicates of both measurements.

of activity remaining in the presence of the compounds. The data presented in Fig. 5 are consistent with previously published literature. The kinase profiling systems allowed the accurate detection of different types of inhibition: (i) specific kinase inhibitors such as tofacitinib, which is a potent and selective JAK3 inhibitor approved for rheumatoid arthritis [9]; (ii) family selective inhibitors such as gefitinib, which targets EGFR and HER2 in the family of ErbB kinases [39], or dasatinib, whose main targets are ABL kinase and the SRC family, along with several other tyrosine kinases, but not ErbB family kinases such as EGFR and HER2 [40]. Moreover, the profiling systems also distinguished inhibition nuances between selective and potent kinase subfamily inhibitors such as dasatinib and less potent but very selective subfamily inhibitors such as roscovitine. Roscovitine is very selective for a number of cyclin-dependent kinases (CDKs) but with less potency than the tyrosine kinase inhibitors described above [41]. As a control for our validation experiment, the p38 MAPK specific inhibitor SB203580 [42,43] was used and no inhibition was observed with the non-target kinases used.

To validate the profiling system for dose–response inhibition, the p38 MAPK family selective inhibitor SB203580 was used to identify the IC_{50} rank order among 16 different CMGC family kinases and more specifically in the p38 kinase subfamily. A dose–response profiling protocol described in Fig. S2 was applied here to generate IC_{50} data for each kinase that are consistent with published literature [42] (Fig. 6A). SB203580 was more potent against the target kinases p38α (IC_{50}: 16 nM) and p38β (IC_{50}: 114 nM) than the other p38 kinases. Other members of the CMGC family were either not inhibited (p38γ, δ, ERK2, and CDKs) or weakly inhibited (JNK1, JNK3, and GSK3β IC_{50} values = 3.3, 0.5, and 1.5 µM, respectively). These results validate the robustness and practicality of our kinase profiling strip concept in accurately identifying kinase inhibitors and potencies.

Kinase inhibitor profiling for 112 kinases

The profiling strip approach proved to be useful for quick kinase inhibitor profiling for small kinase panels. To validate these profiling systems with a larger kinase panel, all 112 kinases in the 14 strips were used in one experimental setup. We adopted two strips per 384-well plate for a total of seven plates and followed the protocol for dose–response inhibitor profiling (Fig. S2). The approach was simple enough for all solution dispensing to be done manually. Seven replicate plates containing compound serial dilutions were created by dispensing 1 µl of pre-prepared SB203580 serial dilution stocks. Next, using two different kinase strips per plate, kinase and substrate stock solutions were dispensed and the plates were incubated before kinase activities were detected using the bioluminescent ADP detection assay. To simplify data analysis when large data sets are generated, worksheets (SMART protocols at http://www.promega.com/resources/tools/) were created in Microsoft Excel for calculating IC_{50} values according to a published method [44]. To easily visualize the SB203580 inhibition profile of the 112-kinase panel, we created a bubble plot on the kinome

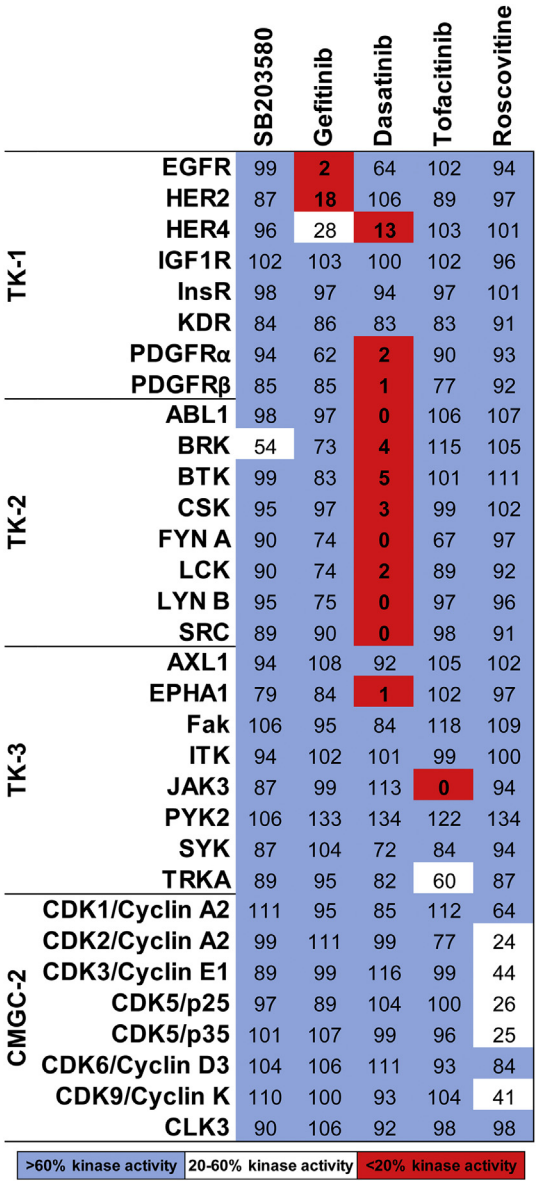

Fig.5. Validation of the strip approach for single-dose inhibitor profile creation. A total of 32 kinases from four different kinase strips were profiled against five kinase inhibitors (1 μM) at once using the single-dose inhibition protocol described in Fig. S1 of the supplementary material. One 384-well plate column was used for each compound/kinase strip pair reaction, one column was used for no-enzyme controls (0% kinase activity), and one column was used for no-compound controls (100% kinase activity). The percentages of activity remaining for kinase/compound pairs are shown and represent the averages of two replicates. Data were collected using the single-dose SMART protocol (http://www.promega.com/resources/tools/), which calculates the percentage kinase activity by subtracting the no-enzyme control luminescence from all kinase-containing reactions and then converting the net luminescence values to percentage activity based on the no-compound control reactions.

image where bubbles represent IC_{50} values for all of the kinases with size in proportion to potency (Fig. 6B). As predicted, the data in Fig. 6B and Table 3 show that SB203580 is a potent and selective inhibitor for both p38α and p38β. We were able to identify an off-target kinase RIPK2 from a different kinome branch (TKL). RIPK2 was potently inhibited with an IC_{50} of 46 nM, which is closer to p38α (IC_{50} = 16 nM) than the other inhibited CMGC kinases such as p38β and JNK3 (Fig. 6A and B and Table 3). RIPK2 was confirmed to be inhibited by SB203580 with a similar IC_{50} in a separate dose–response experiment (data not shown), and this has also been reported in the literature [45].

For a quick assessment of the overall selectivity of a small number of compounds identified during compound library screening, it is useful to perform a single-dose inhibitor profiling. To validate our approach for this purpose with a large kinase panel in a single-dose profiling, 112 kinases were used in one experimental setup with six compounds. We adopted three strips per each 384-well plate for a total of 5 plates. The remaining kinase activity for the 112 kinases in response to 1-μM inhibitor treatments is presented as a heat map in Fig. 7 (right panel). As shown previously, all of the specific and family inhibitions were confirmed. In addition, off-target activity of SB203580 on RIPK2 was confirmed. Interestingly, RIPK2 was also inhibited by gefitinib and dasatinib, which are tyrosine kinase family inhibitors. RIPK2 inhibition by these two inhibitors has also been reported in the literature [23,45].

Many useful features of a convenient profiling approach have been described here, showing that once profiling strips are made and stored, compound selectivity assessments can be routinely performed. This approach saves time, and because of its flexibility it can be used in various stages of kinase drug discovery. For example, numerous hits from high-throughput screening (HTS) can be tested simultaneously for selectivity in single-dose mode, or a few lead compounds can be assessed for their potency in dose–response mode across a large kinase panel. Although 112 kinases constitute good coverage of the kinome and provide a general view of inhibitor selectivity, one shortcoming for the selected panel is that the inhibition of some of the kinases not represented might be missed.

Comparison of bioluminescent and radioactive kinase inhibitor profiling

Radioactivity-based methods are considered the “gold standard” for many detection assays. However, additional assay formats such as fluorescence, luminescence, and absorbance have been developed. When used for kinase activity detection, these systems have some advantages such as ease of use, safety, and homogeneous formats making them HTS friendly. But some nonradioactive approaches have drawbacks such us high false positive rates due to compound fluorescence or absorbance, low sensitivity, and requirements for modified substrates or different antibodies for each assay [46]. Previously, we and others have shown that bioluminescent ADP detection-based kinase assays are similar to radioactive assays in sensitivity and IC_{50} determinations [19,47]. We needed to validate the data generated by the kinase profiling strips approach by comparing the inhibition values obtained with previously published profiling data. Several approaches were used for generating large biochemical-based kinase profiling maps, measuring either the binding of the small molecule to the kinases [24,48–50] or the inhibition of kinase catalytic activity [23,26,27]. Here, we chose to compare profiling strip data with a radioactive method because both assays are based on biochemical kinase activity detection. A common radiometric approach is based on filter binding where the kinase reaction is performed in the presence of [γ-^{32}P]ATP or [γ-^{33}P]ATP, followed by binding of the radioactive product to filters. This technique requires washing to eliminate unbound radioactive material before quantification. Because of the washing steps and safety concerns associated with radioisotope handling, these technologies are not homogeneous and are unattractive to many researchers for large-scale kinase screening or profiling. However, corporations such as Reaction Biology and EMD Millipore do offer large-scale kinase profiling using radiometric assays as a fee for service. Anastassiadis and coworkers described one of the largest profiling data sets using the

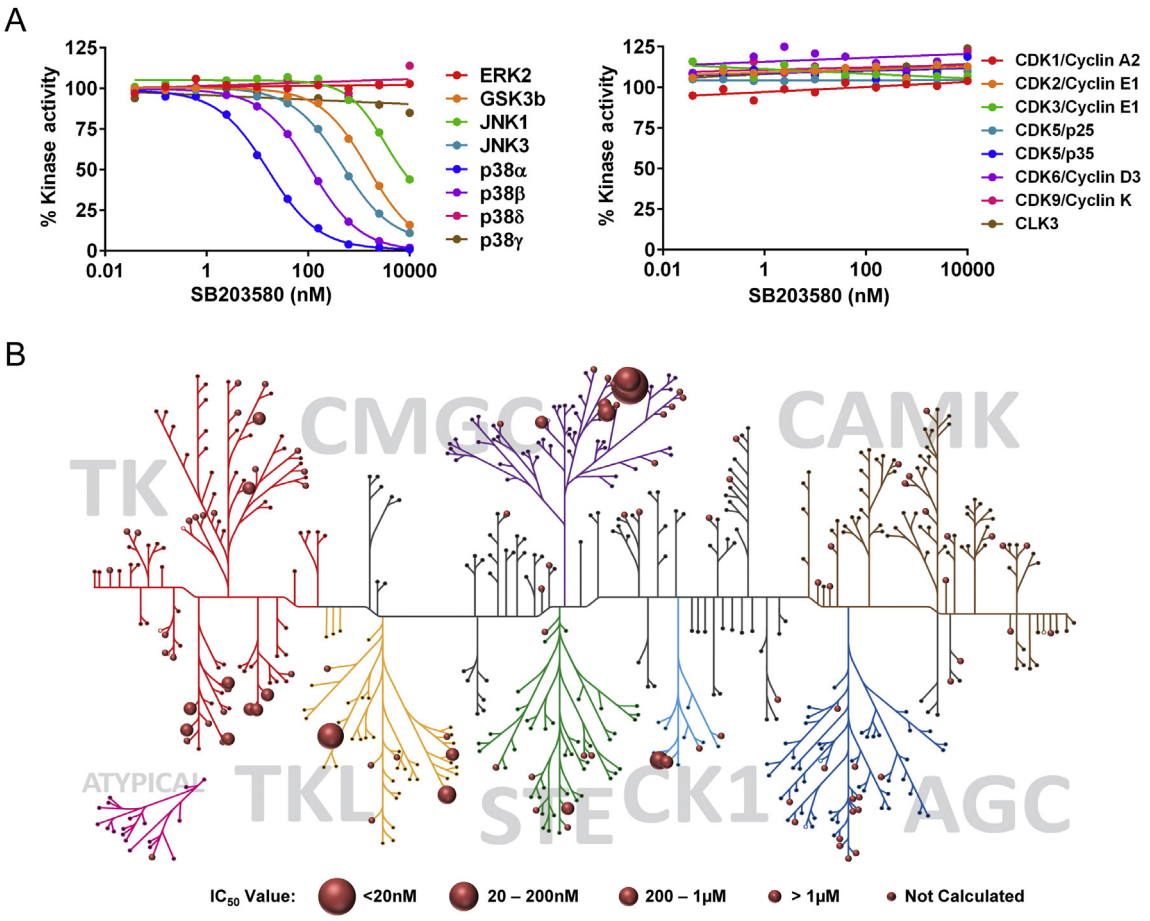

Fig.6. Validation of the strip approach for dose–response inhibitor profile creation. (A) The p38 kinase inhibitor SB203580 was tested on two CMGC kinase strips in 10-point inhibitor dose response as described previously and in Fig. S2 of the Supplementary Material. Curves were fit to a sigmoidal dose–response (variable slope) equation using the dose–response SMART protocol (http://www.promega.com/resources/tools/). The percentages of activity remaining for kinases are shown and represent the averages of two replicates. (B) Profiling the SB203580 compound against the 112-kinase panel using the strip approach. Using the dose–response SMART protocol, IC_{50} values for kinases were collected and converted in Microsoft Excel to different size bubbles to represent the potency of the compound against the kinases.

radiometric HotSpot technology offered by a service provider [23]. A panel of 300 recombinant protein kinases was used with a library of 178 compounds. Only 106 kinases from our panel were profiled in the radiometric panel. Therefore, we compared the data generated with our panel for six compounds with the data generated using the radiometric assay for those 106 kinases. The heat map comparison in Fig. 7 shows good correlation between bioluminescent profiling strip data and the HotSpot data. Indeed, more than 95% of the inhibition values fall within the same range of activity. Because our assay was performed at 1 μM compound concentration compared with 0.5 μM for the radiometric assay, a few kinases show a slight shift in inhibition profile either from high activity remaining (blue) to medium activity (white) or from medium activity remaining (white) to low activity (red). An example of the latter is RIPK2, whose inhibition by three of the small molecules tested was also confirmed. The observed close correlation to a radiometric kinase assay method reinforces the validation of the profiling strips method to generate accurate inhibitor profiles in an uncomplicated fashion. By using the bioluminescent approach to generate profiling data, we eliminated undesirable aspects associated with the use of radioactivity or outsourcing.

Table 3
IC_{50} values calculated for SB203580 toward the kinases in the panel.

Kinase[a]	IC_{50} (nM)
p38α	16
RIPK2	46
p38β	114
JNK3	466
ALK4	853
CK1ε	937
BRK	1334
TNIK	1382
GSK3β	1513
HER2	2081
CK1α1	3007
RET	3219
JNK1	3272
ALK2	4872
HER4	5053
FGFR1	7271

[a] For the rest of the kinases, no IC_{50} could be calculated because the compound had no detectable potency.

Simultaneous profiling of protein and lipid kinases

A desirable component of a simple profiling technique is an assay that detects the activity of all the kinases simultaneously. Lipid kinases have special requirements for assay development due to the intricate nature of the lipid substrates. Therefore,

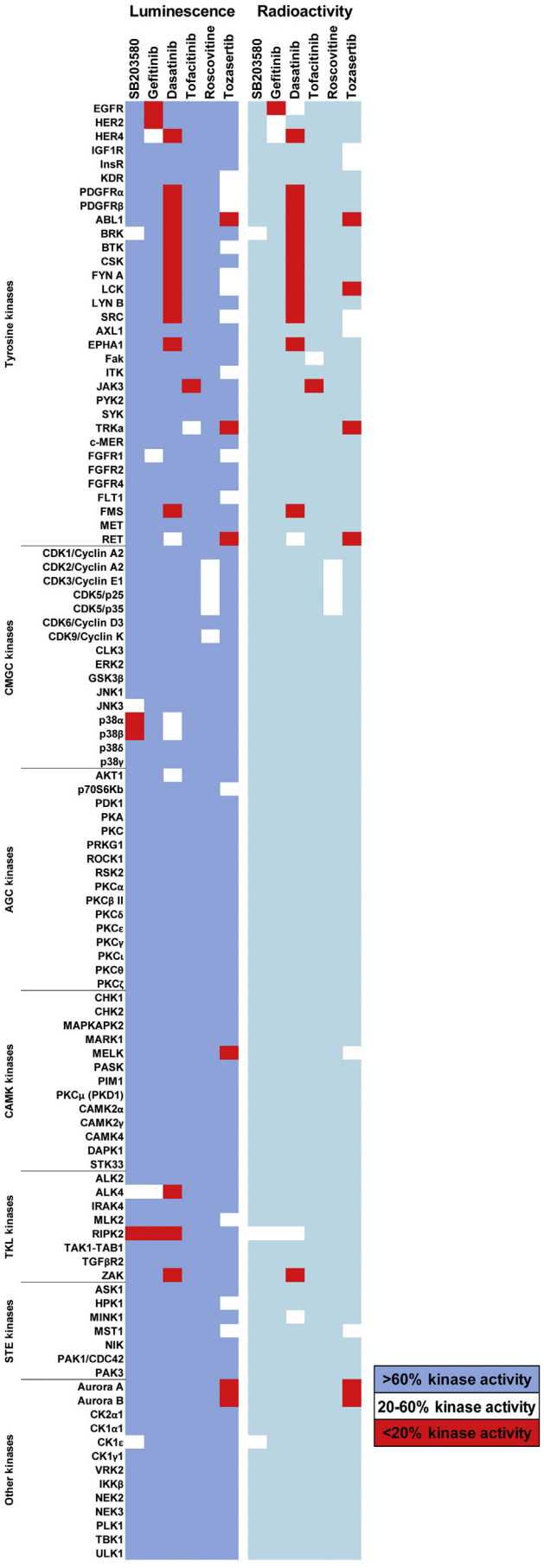

specific assays are used to assess their activities, making them difficult to be included with protein kinases in one setup. This is not an issue when using the luminescent ADP detection assay given that it was previously validated for its robustness and accuracy in detecting the activity of lipid kinases such as PI3 and PI4 kinases [47,51]. We applied our kinase standardizing approach to lipid kinases and created a strip containing the PI3 kinases α, β, γ, and δ. The PI3K strip was used along with the "Other/CK1" strip containing protein kinases from the CK1, the "Other" kinome branch, and DNA-PK. We analyzed the activity of four known PI3K inhibitors: broad-spectrum PI3K inhibitor LY294002, specific PI3Kβ inhibitor AZD6482, and two PI3Kγ inhibitors AS252424 and AS605240. The inhibition profiles of these inhibitors are presented in Fig. 8, and the IC_{50} values generated are shown in Table S2 of the Supplementary Material. All four inhibitors are active with different potencies and different IC_{50} ranges against all of the PI3 kinases. An exception is AS252424, which inhibits the target PI3Kγ with a low IC_{50} of 52 nM and the other PI3 kinases with high IC_{50} but does not inhibit PI3Kβ (Fig. 8D). DNA-PK, which belongs to the same "ATYPICAL" kinome branch as the PI3 kinases (Fig. 1), was also inhibited, as was previously shown by AZD6482 and LY294002 compounds [52]. We found that AS605240 showed the highest potency against DNA-PK with an IC_{50} of 16.3 nM, which is within the same range to its PI3Kγ inhibition (6.4 nM) that this compound is known to be selective for (Fig. 8C and Table S2). The IC_{50} values obtained and the rank orders for these inhibitors are also similar to those in previous reports [52–54]. Surprisingly, we found that in the "Other/CK1" family the protein kinase CK2 was inhibited by AS605240 and AS252424 with potencies similar to that for PI3Kγ (Fig. 8C and D). AS252424 was previously reported to inhibit CK2 with no discussion from the authors of the report about a potential effect on the CK2 pathway [54]. AS605240 was not reported to inhibit CK2. Both compounds were reported to specifically inhibit the PI3Kγ pathway, leading to conclusions that these compounds could have potential application in the treatment of PI3K-mediated chronic inflammatory diseases such as glomerulonephritis [55–57]. CK2 phosphorylates hundreds of substrates and potentially participates in the regulation of diverse cellular processes [58]. During recent years, this ubiquitous kinase was also shown to be involved in inflammation [59,60]. Our finding that CK2 is highly inhibited by these PI3Kγ compounds suggests that the effects observed on the regulation of inflammatory responses could be attributed to CK2 or could synergistically involve both the PI3Kγ and CK2 pathways [55,60]. This emphasizes the importance of including lipid and protein kinases in profiling experiments to rule out any misinterpretations or erroneous conclusions related to the effects of compounds at the cellular level.

We have shown here that lipid kinases can also be assembled in strip format to be used with protein kinases in the same profiling experiments. Profiling these kinases in strips easily identifies compound selectivity toward members of the PI3 kinase family and defines rank orders. Finally, because compounds were profiled simultaneously against lipid and protein kinases, unknown off-

Fig.7. Comparison of large selectivity profiles generated with the luminescent and radiometric approaches. Right panel: A total of 106 kinases from the kinase strips panel were tested in the luminescent method described here against six compounds known for their specific inhibition profiles at 1 μM concentration. The single-dose inhibition protocol and data collection were performed as described in Fig. 3. Percentages of activity remaining for kinase/compound pairs are shown as a heat map representing different kinase activity ranges. Left panel: Data produced by a radiometric assay [23] for the same 106 kinases was collected from the publication and converted to a heat map for comparison with the luminescent approach.

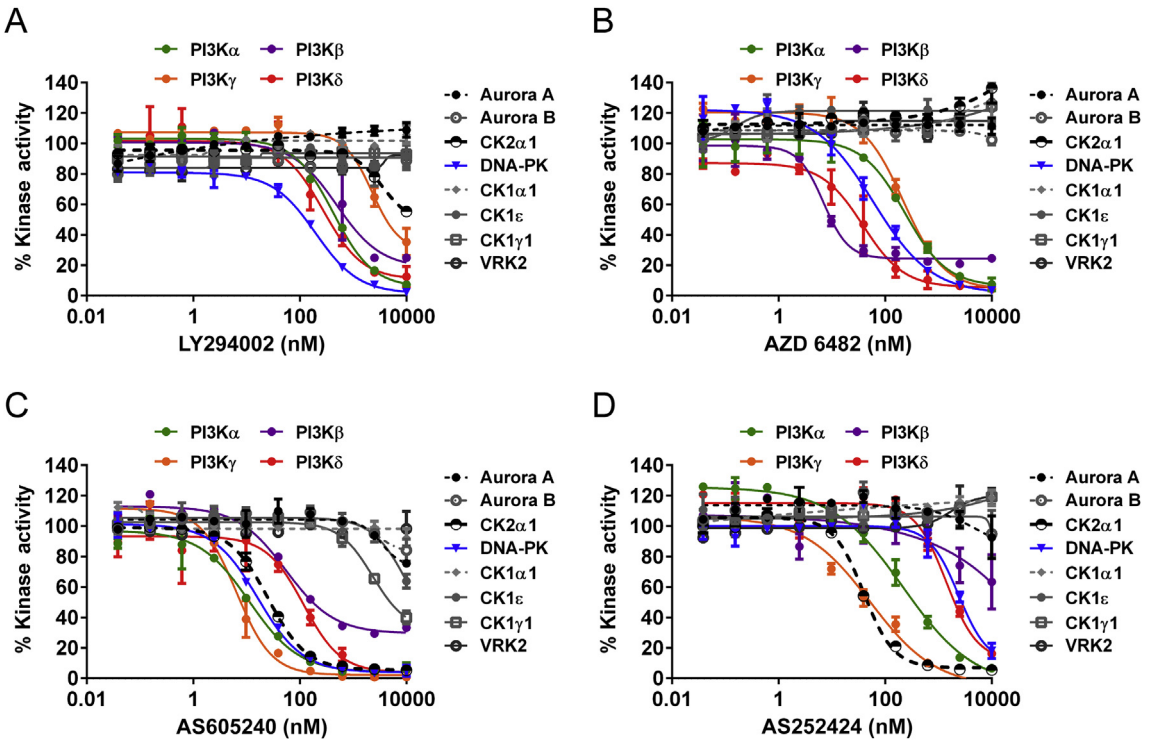

Fig.8. Selectivity profiling of PI3 kinase inhibitors. Lipid kinase inhibitors LY294002 (A), AZD 6482 (B), AS605240 (C), and AS252424 (D) were profiled against PI3 kinases and selected protein kinases simultaneously using the strip approach. To have the 12 kinases together in one graph, curves were fit to a sigmoidal dose–response (variable slope) equation using GraphPad Prism software. The percentages of activity remaining for kinase/compound pairs are shown and represent the averages of two replicates. IC_{50} values calculated are presented in Table S2 of the Supplementary Material.

target effects that would have been missed otherwise were identified.

Conclusions

During drug development, profiling kinase inhibitors is a crucial step that allows medicinal chemists to pursue lead compound optimization and dial in a good balance between potency and selectivity. Early and iterative availability of this information during the optimization process supports the development of efficacious drugs with minimal side effects later in the clinic and lowers the attrition rate of drug candidates. Many techniques are available to assess the potency of an inhibitor on kinase activity. However, to assess selectivity of a compound, there are many challenges that can be encountered. First, to perform a profiling experiment, multiple kinases need to be assayed at the same time, and one kinase assay method might not be suitable for all of them. This challenge can be overcome with a generic assay that detects the activity of all kinases regardless of the nature of their substrates. We accomplished this in the current examples with an assay that measures production of the universal kinase product ADP. Second, assay development for each kinase in the profiling panel and the maintenance of kinase enzyme stability and supply can be challenging. We overcame this challenge by developing a simple bioluminescent profiling platform based on the functional ADP detection assay. Our method relies on standardizing kinase activities and creating pre-configured kinase stocks that are used in kinase reactions to create either inhibitor single-dose or dose–response profiles. Our method provides a simple but powerful tool to streamline the profiling process and routinely generate profiling data in an uncomplicated manner. The data generated by this new approach are comparable to previously reported methods without the associated technical challenges such as heavy assay development, safety due to radioactive material management, and inconveniences related to outsourcing. We showed that by using the kinase profiling strip approach, we could easily generate selectivity profiles with either small or large kinase panels. This novel approach can be easily adopted by scientists such as medicinal chemists and chemical biologists for regular in-house kinase inhibitor profiling.

Acknowledgments

We thank Jim Cali for his critical reading of the manuscript, Vincent Lee for helping with kinase strip assembly, Jun Yan for kindly providing enzymes, Mark Bratz for creating the SMART protocol data analysis tool, and Michael Stormberg for creating the kinome dendogram image. The authors are former or current employees of Promega Corporation or Signalchem Pharmaceuticals.

Appendix A. Supplementary data

Supplementary data related to this article can be found at http://dx.doi.org/10.1016/j.ab.2015.11.007.

References

[1] G. Manning, D.B. Whyte, R. Martinez, T. Hunter, S. Sudarsanam, The protein kinase complement of the human genome, Science 298 (2002) 1912–1934.
[2] P.V. Hornbeck, J.M. Kornhauser, S. Tkachev, B. Zhang, E. Skrzypek, B. Murray, V. Latham, M. Sullivan, PhosphoSitePlus: a comprehensive resource for investigating the structure and function of experimentally determined post-translational modifications in man and mouse, Nucleic Acids Res. 40 (2012) D261–D270.
[3] T. Hunter, Signaling—2000 and beyond, Cell 100 (2000) 113–127.
[4] P. Cohen, Protein kinases—–the major drug targets of the twenty-first century? Nat. Rev. Drug Discov. 1 (2002) 309–315.

[5] P. Cohen, D.R. Alessi, Kinase drug discovery: what's next in the field? ACS Chem. Biol. 8 (2013) 96–104.
[6] P. Wu, T.E. Nielsen, M.H. Clausen, FDA-approved small-molecule kinase inhibitors, Trends Pharmacol. Sci. 36 (2015) 422–439.
[7] M.H. Cohen, G. Williams, J.R. Johnson, J. Duan, J. Gobburu, A. Rahman, K. Benson, J. Leighton, S.K. Kim, R. Wood, M. Rothmann, G. Chen, K. Maung-U, A.M. Staten, R. Pazdur, Approval summary for imatinib mesylate capsules in the treatment of chronic myelogenous leukemia, Clin. Cancer Res. 8 (2002) 935–942.
[8] A. Ganetsky, Ruxolitinib: a new treatment option for myelofibrosis, Pharmacotherapy 33 (2013) 84–92.
[9] E.B. Lee, R. Fleischmann, S. Hall, B. Wilkinson, J.D. Bradley, D. Gruben, T. Koncz, S. Krishnaswami, G.V. Wallenstein, C. Zang, S.H. Zwillich, R.F. van Vollenhoven, Tofacitinib versus methotrexate in rheumatoid arthritis, N. Engl. J. Med. 370 (2014) 2377–2386.
[10] L. Richeldi, R.M. du Bois, G. Raghu, A. Azuma, K.K. Brown, U. Costabel, V. Cottin, K.R. Flaherty, D.M. Hansell, Y. Inoue, D.S. Kim, M. Kolb, A.G. Nicholson, P.W. Noble, M. Selman, H. Taniguchi, M. Brun, F. Le Maulf, M. Girard, S. Stowasser, R. Schlenker-Herceg, B. Disse, H.R. Collard, Efficacy and safety of nintedanib in idiopathic pulmonary fibrosis, N. Engl. J. Med. 370 (2014) 2071–2082.
[11] C. Widakowich, G. de Castro, E. de Azambuja, P. Dinh, A. Awada, Review: Side effects of approved molecular targeted therapies in solid cancers, Oncologist 12 (2007) 1443–1455.
[12] P.J. Barnes, New anti-inflammatory targets for chronic obstructive pulmonary disease, Nat. Rev. Drug Discov. 12 (2013) 543–559.
[13] M. Rask-Andersen, J. Zhang, D. Fabbro, H.B. Schiöth, Advances in kinase targeting: current clinical use and clinical trials, Trends Pharmacol. Sci. 35 (2014) 604–620.
[14] R.E. Castoldi, G. Pennella, G.S. Saturno, P. Grossi, M. Brughera, M. Venturi, Assessing and managing toxicities induced by kinase inhibitors, Curr. Opin. Drug Discov. Dev. 10 (2007) 53–57.
[15] A.J. Olaharski, N. Gonzaludo, H. Bitter, D. Goldstein, S. Kirchner, H. Uppal, K. Kolaja, Identification of a kinase profile that predicts chromosome damage induced by small molecule kinase inhibitors, PLoS Comput. Biol. 5 (7) (2009) e1000446.
[16] J. Bain, L. Plater, M. Elliott, N. Shpiro, C.J. Hastie, H. Mclauchlan, I. Klevernic, J. Simon, C. Arthur, D.R. Alessi, P. Cohen, The selectivity of protein kinase inhibitors: a further update, Biochem. J. 408 (2007) 297–315.
[17] Y. Hu, N. Furtmann, J. Bajorath, Current compound coverage of the kinome, J. Med. Chem. 58 (2015) 30–40.
[18] Y. Jia, C.M. Quinn, S. Kwak, R.V. Talanian, Current in vitro kinase assay technologies: the quest for a universal format, Curr. Drug Discov. Technol. 5 (2008) 59–69.
[19] H. Zegzouti, M. Zdanovskaia, K. Hsiao, S.A. Goueli, ADP-Glo: a bioluminescent and homogeneous ADP monitoring assay for kinases, assay, Drug Dev. Technol. 7 (2009) 560–572.
[20] R. Krishnamurty, D.J. Maly, Chemical genomic and proteomic methods for determining kinase inhibitor selectivity, Comb. Chem. High. Throughput Screen 10 (2007) 652–666.
[21] Y. Luo, Selectivity assessment of kinase inhibitors: strategies and challenges, Curr. Opin. Mol. Ther. 7 (2005) 251–255.
[22] C.V. Miduturu, X. Deng, N. Kwiatkowski, W. Yang, L. Brault, P. Filippakopoulos, E. Chung, Q. Yang, J. Schwaller, S. Knapp, R.W. King, J.-D. Lee, S. Herrgard, P. Zarrinkar, N.S. Gray, High-throughput kinase profiling: a more efficient approach towards the discovery of new kinase inhibitors, Chem. Biol. 18 (2011) 868–879.
[23] T. Anastassiadis, S.W. Deacon, K. Devarajan, H. Ma, J.R. Peterson, Comprehensive assay of kinase catalytic activity reveals features of kinase inhibitor selectivity, Nat. Biotechnol. 29 (2011) 1039–1045.
[24] M.A. Fabian, W.H. Biggs, D.K. Treiber, C.E. Atteridge, M.D. Azimioara, M.G. Benedetti, T.A. Carter, P. Ciceri, P.T. Edeen, M. Floyd, J.M. Ford, M. Galvin, J.L. Gerlach, R.M. Grotzfeld, S. Herrgard, D.E. Insko, M.A. Insko, A.G. Lai, J.-M. Lelias, S.A. Mehta, Z.V. Milanov, A.M. Velasco, L.M. Wodicka, H.K. Patel, P.P. Zarrinkar, D.J. Lockhart, A small molecule–kinase interaction map for clinical kinase inhibitors, Nat. Biotechnol. 23 (2005) 329–336.
[25] M.W. Karaman, S. Herrgard, D.K. Treiber, P. Gallant, C.E. Atteridge, B.T. Campbell, K.W. Chan, P. Ciceri, M.I. Davis, P.T. Edeen, R. Faraoni, M. Floyd, J.P. Hunt, D.J. Lockhart, Z.V. Milanov, M.J. Morrison, G. Pallares, H.K. Patel, S. Pritchard, L.M. Wodicka, P.P. Zarrinkar, A quantitative analysis of kinase inhibitor selectivity, Nat. Biotechnol. 26 (2008) 127–132.
[26] Y. Gao, S.P. Davies, M. Augustin, A. Woodward, U.A. Patel, R. Kovelman, K.J. Harvey, A broad activity screen in support of a chemogenomic map for kinase signalling research and drug discovery, Biochem. J. 451 (2013) 313–328.
[27] D. Kitagawa, K. Yokota, M. Gouda, Y. Narumi, H. Ohmoto, E. Nishiwaki, K. Akita, Y. Kirii, Activity-based kinase profiling of approved tyrosine kinase inhibitors, Genes Cells 18 (2013) 110–122.
[28] A. Card, C. Caldwell, H. Min, B. Lokchander, H. Xi, S. Sciabola, A.V. Kamath, S.L. Clugston, W.R. Tschantz, L. Wang, D.J. Moshinsky, High-throughput biochemical kinase selectivity assays: panel development and screening applications, J. Biomol. Screen 14 (2009) 31–42.
[29] B. Larson, P. Banks, H. Zegzouti, S.A. Goueli, A simple and robust automated kinase profiling platform using luminescent ADP accumulation technology, assay, Drug Dev. Technol. 7 (2009) 573–584.
[30] H. Zegzouti, J. Alves, T. Worzella, G. Vidugiris, G. Cameron, J. Vidugiriene, S. Goueli, Screening and Profiling Kinase Inhibitors With a Luminescent ADP Detection Platform, Promega, 2011. Available from: http://www.promega.com/resources/pubhub/screening-and-profiling-kinase-inhibitors-with-a-luminescent-adp-detection-platform/.
[31] C. Tanega, M. Shen, B.T. Mott, C.J. Thomas, R. MacArthur, J. Inglese, D.S. Auld, Comparison of bioluminescent kinase assays using substrate depletion and product formation, assay, Drug Dev. Technol. 7 (2009) 606–614.
[32] S.B. Berger, P. Harris, R. Nagilla, V. Kasparcova, S. Hoffman, B. Swift, L. Dare, M. Schaeffer, C. Capriotti, M. Ouellette, B.W. King, D. Wisnoski, J. Cox, M. Reilly, R.W. Marquis, J. Bertin, P.J. Gough, Characterization of GSK'963: a structurally distinct, potent, and selective inhibitor of RIP1 kinase, Cell Death Discov. 1 (2015) 15009, http://dx.doi.org/10.1038/cddiscovery.2015.9.
[33] C. Antczak, A. Bermingham, P. Calder, D. Malkov, K. Song, J. Fetter, H. Djaballah, Domain-based biosensor assay to screen for epidermal growth factor receptor modulators in live cells, assay, Drug Dev. Technol. 10 (2012) 24–36.
[34] S.K.C. Basnet, S. Diab, R. Schmid, M. Yu, Y. Yang, T.A. Gillam, T. Teo, P. Li, T. Peat, H. Albrecht, S. Wang, Identification of a highly conserved allosteric binding site on Mnk1 and Mnk2, Mol. Pharmacol. 88 (2015) 935–948.
[35] T. Luo, K. Masson, J.D. Jaffe, W. Silkworth, N.T. Ross, C.A. Scherer, C. Scholl, S. Fröhling, S.A. Carr, A.M. Stern, S.L. Schreiber, T.R. Golub, STK33 kinase inhibitor BRD-8899 has no effect on KRAS-dependent cancer cell viability, Proc. Natl. Acad. Sci. U. S. A. 109 (2012) 2860–2865.
[36] S. Santaguida, C. Vernieri, F. Villa, A. Ciliberto, A. Musacchio, Evidence that Aurora B is implicated in spindle checkpoint signalling independently of error correction, EMBO J. 30 (2011) 1508–1519.
[37] H. Zegzouti, J. Hennek, S. Goueli, Using bioluminescent kinase profiling strips to identify inhibitor selectivity and promiscuity, Methods Mol. Biol. 1360 (2016) 59–73.
[38] D.K. Heidary, G. Huang, D. Boucher, J. Ma, C. Forster, R. Grey, J. Xu, M. Arnost, D. Choquette, G. Chen, J.-H. Zhou, Y.-M. Yao, E.D. Ball, M. Namchuk, R.J. Davies, G. Henkel, VX-322: a novel dual receptor tyrosine kinase inhibitor for the treatment of acute myelogenous leukemia, J. Med. Chem. 55 (2012) 725–734.
[39] C-H. Yun, T.J. Boggon, Y. Li, M.S. Woo, H. Greulich, M. Meyerson, M.J. Eck, Structures of lung cancer-derived EGFR mutants and inhibitor complexes: mechanism of activation and insights into differential inhibitor sensitivity, Cancer Cell 11 (2007) 217–227.
[40] M. Steinberg, Dasatinib: a tyrosine kinase inhibitor for the treatment of chronic myelogenous leukemia and philadelphia chromosome-positive acute lymphoblastic leukemia, Clin. Ther. 29 (2007) 2289–2308.
[41] S. Bach, M. Knockaert, J. Reinhardt, O. Lozach, S. Schmitt, B. Baratte, M. Koken, S.P. Coburn, L. Tang, T. Jiang, D.-C. Liang, H. Galons, J.-F. Dierick, L.A. Pinna, F. Meggio, F. Totzke, C. Schächtele, A.S. Lerman, A. Carnero, Y. Wan, N. Gray, L. Meijer, Roscovitine targets, protein kinases, and pyridoxal kinase, J. Biol. Chem. 280 (2005) 31208–31219.
[42] A. Cuenda, J. Rouse, Y.N. Doza, R. Meier, P. Cohen, T.F. Gallagher, P.R. Young, J.C. Lee, SB 203580 is a specific inhibitor of a MAP kinase homologue which is stimulated by cellular stresses and interleukin-1, FEBS Lett. 364 (1995) 229–233.
[43] S. Kumar, M.S. Jiang, J.L. Adams, J.C. Lee, Pyridinylimidazole compound SB 203580 inhibits the activity but not the activation of p38 mitogen-activated protein kinase, Biochem. Biophys. Res. Commun. 263 (1999) 825–831.
[44] J.D. Parsons, A high-throughput method for fitting dose–response curves using Microsoft Excel, Anal. Biochem. 360 (2007) 309–311.
[45] J.T. Tigno-Aranjuez, P. Benderitter, F. Rombouts, F. Deroose, X. Bai, B. Mattioli, F. Cominelli, T.T. Pizarro, J. Hoflack, D.W. Abbott, In vivo inhibition of RIPK2 kinase alleviates inflammatory disease, J. Biol. Chem. 289 (2014) 29651–29664.
[46] H. Ma, S. Deacon, K. Horiuchi, The challenge of selecting protein kinase assays for lead discovery optimization, Expert Opin. Drug Discov. 3 (2008) 607–621.
[47] A.W. Tai, N. Bojjireddy, T. Balla, A homogeneous and nonisotopic assay for phosphatidylinositol 4-kinases, Anal. Biochem. 417 (2011) 97–102.
[48] M.I. Davis, J.P. Hunt, S. Herrgard, P. Ciceri, L.M. Wodicka, G. Pallares, M. Hocker, D.K. Treiber, P.P. Zarrinkar, Comprehensive analysis of kinase inhibitor selectivity, Nat. Biotechnol. 29 (2011) 1046–1051.
[49] G. Médard, F. Pachl, B. Ruprecht, S. Klaeger, S. Heinzlmeir, D. Helm, H. Qiao, X. Ku, M. Wilhelm, T. Kuehne, Z. Wu, A. Dittmann, C. Hopf, K. Kramer, B. Kuster, Optimized chemical proteomics assay for kinase inhibitor profiling, J. Proteome Res. 14 (2015) 1574–1586.
[50] M.P. Patricelli, T.K. Nomanbhoy, J. Wu, H. Brown, D. Zhou, J. Zhang, S. Jagannathan, A. Aban, E. Okerberg, C. Herring, B. Nordin, H. Weissig, Q. Yang, J.-D. Lee, N.S. Gray, J.W. Kozarich, In situ kinase profiling reveals functionally relevant properties of native kinases, Chem. Biol. 18 (2011) 699–710.
[51] A.W. Tai, J. Vidugiriene, Measuring activity of phosphoinositide lipid kinases using a bioluminescent ADP-detecting assay, Methods Mol. Biol. 1360 (2016) 75–85.
[52] Z.A. Knight, B. Gonzalez, M.E. Feldman, E.R. Zunder, D.D. Goldenberg, O. Williams, R. Loewith, D. Stokoe, A. Balla, B. Toth, T. Balla, W.A. Weiss, R.L. Williams, K.M. Shokat, A pharmacological map of the PI3-K family defines a role for p110α in insulin signaling, Cell 125 (2006) 733–747.
[53] D. Kong, T. Yamori, Phosphatidylinositol 3-kinase inhibitors: promising drug candidates for cancer therapy, Cancer Sci. 99 (2008) 1734–1740.
[54] V. Pomel, J. Klicic, D. Covini, D.D. Church, J.P. Shaw, K. Roulin, F. Burgat-Charvillon, D. Valognes, M. Camps, C. Chabert, C. Gillieron, B. Françon,

D. Perrin, D. Leroy, D. Gretener, A. Nichols, P.A. Vitte, S. Carboni, C. Rommel, M.K. Schwarz, T. Rückle, Furan-2-ylmethylene thiazolidinediones as novel, potent, and selective inhibitors of phosphoinositide 3-kinase γ, J. Med. Chem. 49 (2006) 3857–3871.

[55] D.F. Barber, A. Bartolome, C. Hernandez, J.M. Flores, C. Redondo, C. Fernandez-Arias, M. Camps, T. Ruckle, M.K. Schwarz, S. Rodriguez, C. Martinez-A, D. Balomenos, C. Rommel, A.C. Carrera, PI3Kγ inhibition blocks glomerulonephritis and extends lifespan in a mouse model of systemic lupus, Nat. Med. 11 (2005) 933–935.

[56] M. Camps, T. Ruckle, H. Ji, V. Ardissone, F. Rintelen, J. Shaw, C. Ferrandi, C. Chabert, C. Gillieron, B. Francon, T. Martin, D. Gretener, D. Perrin, D. Leroy, P.-A. Vitte, E. Hirsch, M.P. Wymann, R. Cirillo, M.K. Schwarz, C. Rommel, Blockade of PI3Kγ suppresses joint inflammation and damage in mouse models of rheumatoid arthritis, Nat. Med. 11 (2005) 936–943.

[57] M. Jin, Q. Zhou, E. Lee, S. Dan, H.Q. Duan, D. Kong, AS252424, a PI3Kγ inhibitor, downregulates inflammatory responsiveness in mouse bone marrow-derived mast cells, Inflammation 37 (2014) 1254–1260.

[58] D.W. Litchfield, Protein kinase CK2: structure, regulation, and role in cellular decisions of life and death, Biochem. J. 369 (2003) 1–15.

[59] N.N. Singh, D.P. Ramji, Protein kinase CK2, an important regulator of the inflammatory response? J. Mol. Med. 86 (2008) 887–897.

[60] M. Yamada, S. Katsuma, T. Adachi, A. Hirasawa, S. Shiojima, T. Kadowaki, Y. Okuno, T.-A. Koshimizu, S. Fujii, Y. Sekiya, Y. Miyamoto, M. Tamura, W. Yumura, H. Nihei, M. Kobayashi, G. Tsujimoto, Inhibition of protein kinase CK2 prevents the progression of glomerulonephritis, Proc. Natl. Acad. Sci. U. S. A. 102 (2005) 7736–7741.